PROCEEDINGS OF SPIE

SPIEDigitalLibrary.org/conference-proceedings-of-spie

Progress in high-speed optical links in the 8 to 12µm thermal atmospheric window from the perspective of unipolar quantum technology

Pierre Didier, Hamza Dely, Olivier Spitz, Thomas Bonazzi, Elie Awwad, et al.

Pierre Didier, Hamza Dely, Olivier Spitz, Thomas Bonazzi, Elie Awwad, Etienne Rodriguez, Angela Vasanelli, Carlo Sirtori, Frédéric Grillot, "Progress in high-speed optical links in the 8 to 12µm thermal atmospheric window from the perspective of unipolar quantum technology," Proc. SPIE 12515, Laser Technology for Defense and Security XVIII, 1251507 (15 June 2023); doi: 10.1117/12.2663847

SPIE.

Event: SPIE Defense + Commercial Sensing, 2023, Orlando, Florida, United States

Progress in high-speed optical links in the 8-12 microns thermal atmospheric window from the perspective of unipolar quantum technology

Pierre Didier[1,2,*], Hamza Dely[3], Olivier Spitz[1,5], Thomas Bonazzi[3], Elie Awwad[1], Etienne Rodriguez[3], Angela Vasanelli[3], Carlo Sirtori[3], and Frédéric Grillot[1,4]

[1]LTCI Telecom Paris, Institut Polytechnique de Paris, 19 Place Marguerite Perey, Palaiseau 91120, France
[2]mirSense, Campus Eiffel, Bâtiment E-RDC, 1 rue Jean Rostand, Orsay, 91400, France
[3]Laboratoire de Physique de l'École Normale Supérieure, ENS, Université PSL, CNRS, Sorbonne Université, Université Paris Cité, 24 rue Lhomond, 75005 Paris, France
[4]Center for High Technology Materials, University of New-Mexico, 1313 Goddard SE, Albuquerque, New Mexico 87106, USA
[5]now with CREOL, College of Optics and Photonics, University of Central Florida, Orlando, Florida 32816, USA

ABSTRACT

Lack of critical communication components (external modulators, high-sensitivity detectors, amplifiers) has long hindered the development of high-speed free-space transmission in the 8-12 μm thermal atmospheric window. Unipolar quantum technology has emerged as a game-changer by developing key elements that outperform conventional direct-modulation schemes in terms of performance. In particular, we demonstrated a free-space communication at 30 Gbits/s. High-speed modulation of the 9 µm-wavelength beam from a quantum cascade laser is implemented with a Stark-effect external modulator while fast detection relies on a quantum well infrared photodetector. In between, a multi-pass cell allows increasing the propagation distance to 31 meters.

Keywords: quantum cascade devices, unipolar quantum optoelectronics, mid-infrared modulator, high-speed photonics, free-space communication

1. INTRODUCTION

The 8-12 µm thermal atmospheric window was the first wavelength domain to be investigated for high-speed communication with quantum cascade lasers (QCLs).[1,2] Peculiarities of QCLs, such as the absence of relaxation oscillations, were very promising for direct-modulation communication in structures where the theoretical bandwidth limit can exceed 100 GHz.[3] However, most of the experimental efforts struggled to demonstrate multi-GHz flat electrical bandwidth.[4] Furthermore, unpractical requirements such as liquid nitrogen or multi-stage Peltier cooling hindered the development of such technology. Starting in 2017, there was a renewed interest for QCL mid-infrared free-space communication with the development of room temperature mid-infrared technology. Yet, the maximum data rate in such experimental efforts was not outperforming that of the early experiments.[5] Since then, numerous experimental endeavors have been undertaken to demonstrate mid-infrared free-space transmission. Some of these efforts have concentrated on the direct modulation of mid-infrared semiconductor lasers,[6,7] while others have relied on difference-frequency generation.[8,9] The latter approach is compatible with wavelength multiplexing, thereby enhancing data rates. However, it is limited by the low optical power available in the mid-infrared after down-conversion. On the other hand, QCLs can now output several Watts at room temperature[10] in the 8-12 µm window and new opportunities are offered by novel mid-infrared amplifiers[11] and external modulators, which are more reliable than direct-modulation techniques. With that in mind, Unipolar

Further author information:
P.D.: E-mail: pierre.didier@telecom-paris.fr

Laser Technology for Defense and Security XVIII, edited by Mark Dubinskii, Rita D. Peterson,
Proc. of SPIE Vol. 12515, 1251507 · © 2023 SPIE · 0277-786X · doi: 10.1117/12.2663847

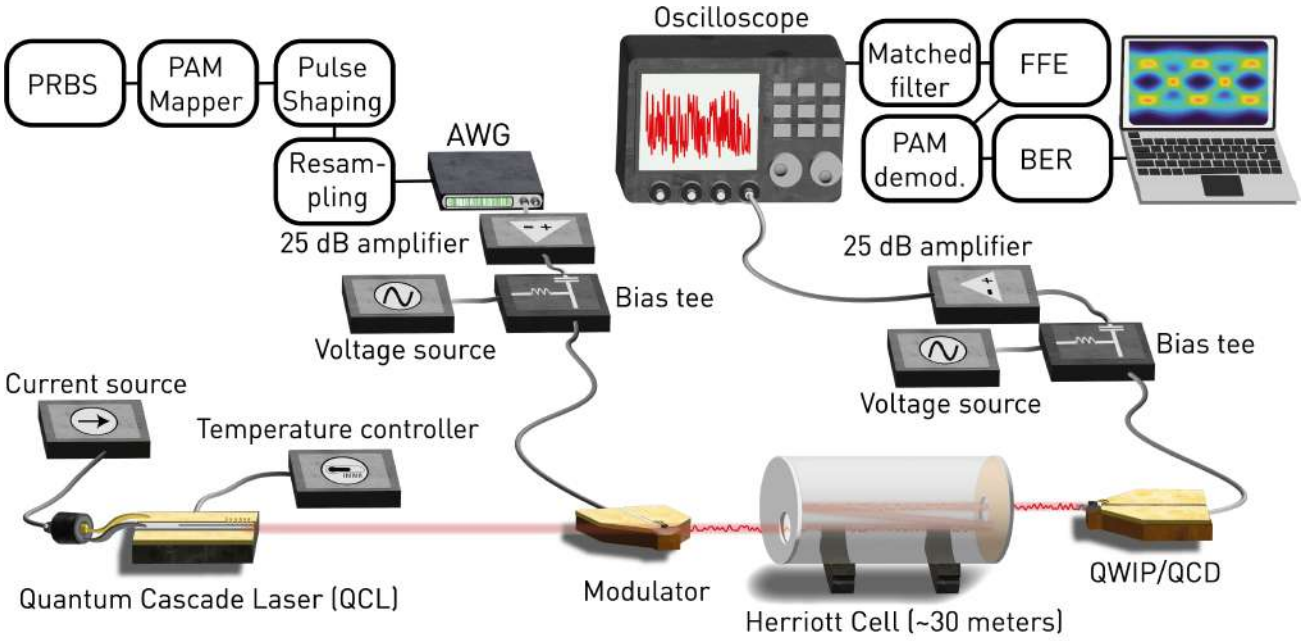

Figure 1. Experimental setup of the high-speed data communication at mid-infrared wavelength. The setup includes three unipolar quantum devices: a quantum cascade laser, an amplitude Stark-effect modulator and a quantum well infrared photodetector (QWIP) connected to a real-time oscilloscope (or alternatively, a quantum cascade detector(QCD) connected to a real-time oscilloscope).

quantum technology[12] is poised to become the candidate of choice for situations where free-space optical communication are easier and faster to implement than conventional fiber networks.

In this work, we present a free-space high-speed transmission using a Stark-effect external modulator[13] optimized for a wavelength of 9µm. The combination of a single-mode QCL with the amplitude Stark-effect modulator and the multi-pass cell allows demonstrating data rate of 14 Gbits/s with a passive quantum cascade detector (QCD) operating at room temperature and a data rate of 30 Gbits/s with a quantum well infrared photodetector (QWIP) operating at the temperature of liquid nitrogen. The total distance of this indoor transmission is 31 meters. Conventional signal pre-processing and post-processing are implemented and enable these multi-Gbit/s transmission rates, with the QWIP-scheme results exceeding the state-of-the-art demonstrations with direct QCL modulation or direct ICL modulation.[14,15] These results provide a path towards wide-scale adoption in relevant free-space telecommunication applications.

2. EXPERIMENTAL SETUP

Figure 1 shows the experimental setup for the free-space communication with a mid-infrared external modulator. This QCL can generate up to 100 mW of optical power on a single mode at 9µm. Wavelength selectivity and high optical power are relevant parameters as the modulator has a narrow optical band of operation and some of the optical power is absorbed by this device. Both the laser and the modulator are operated at room temperature. The mid-infrared beam is focused towards the amplitude Stark-effect modulator that is linked to a custom coplanar waveguide and RF-mounted for high-speed operation. The modulator requires a continuous bias to operate within its linear functional range, along with an AC signal that corresponds to the bit sequence transmission. The characteristics of the optical channel are analyzed prior to message encoding because knowing these characteristics allows adapting the amplitude and frequency allocation of the AC signal. This adaptation is achieved with a Matlab program which outputs a custom trace for the bit sequence and that trace is loaded to the Socionext arbitrary waveform generator (AWG) with a sampling rate of 120 GS/s. The AWG acts as a digital-to-analog converter with a maximum bandwidth of 30 GHz and a maximum peak-to-peak output voltage of 1.5 V. Amplification of the AC signal from the AWG is required to address impedance mismatch between the

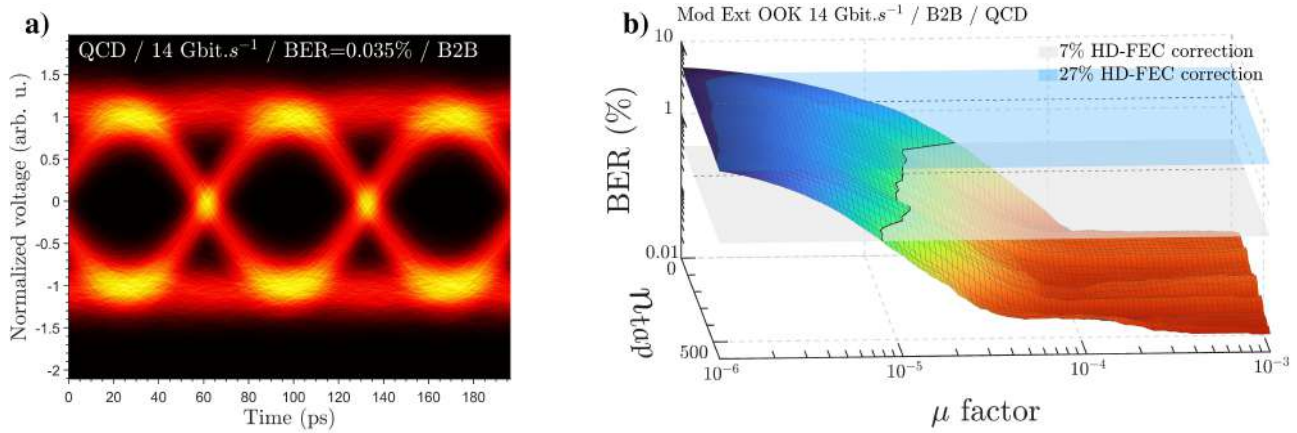

Figure 2. a) Eye diagram of the QCD-scheme transmission after a free-space propagation of approximately 2 meters for an OOK format at 14 Gbit/s, exhibiting an error rate of 0.035 %. b) Optimization of the FFE equalization parameters in order to achieve a BER compatible with either the 27% HD-FEC case or with the 7% HD-FEC case.

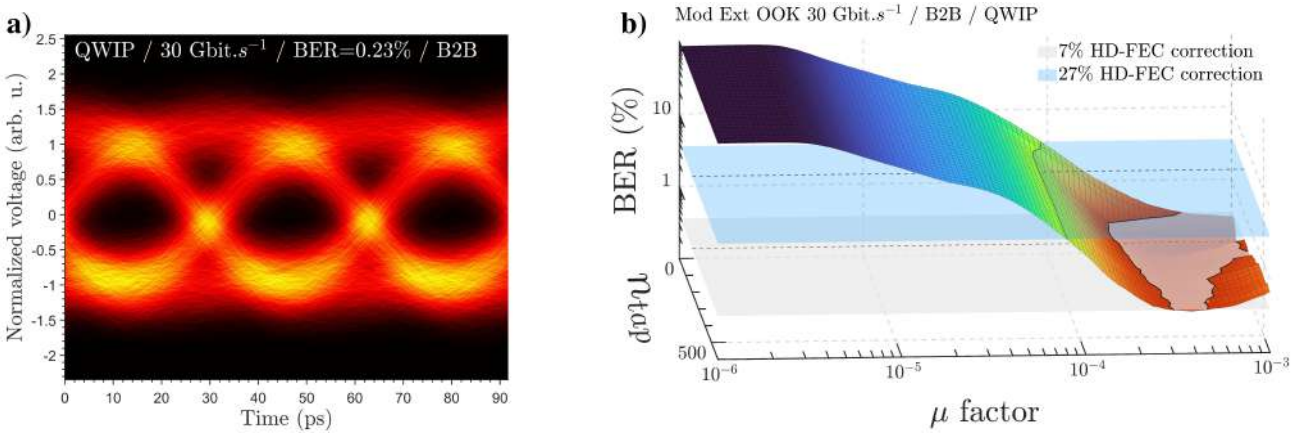

Figure 3. a) Eye diagram of the QWIP-scheme transmission after a free-space propagation of approximately 2 meters for an OOK format at 30 Gbit/s, exhibiting an error rate of 0.23 %. b) Optimization of the FFE equalization parameters in order to achieve a BER compatible with either the 27% HD-FEC case or with the 7% HD-FEC case.

AWG output and the modulator input. As shown in Fig. 1, the modulator imprints the message on the mid-infrared carrier. This amplitude-modulated mid-infrared wave travels 31 meters before impinging either a room-temperature quantum cascade detector (QCD) or a cryogenic quantum well infrared photodetector (QWIP), and those are also RF-mounted for high-speed operation. The 31-meter table-top propagation is achieved thanks to a multi-pass cell (Thorlabs, HC30L-M02). The high-speed detector allows photonics-to-electrical conversion to get rid of the mid-infrared carrier. This electrical signal, corresponding to the transmitted message, is amplified and recorded by a real-time oscilloscope (Tektronix, DPO70000SX) at a sampling rate of 100 GS/s. The recorded signal is then post-processed with steps including resampling at a constant sampling per symbol and feed-forward equalization (FFE). The last step is to compare the received bit sequence with the initial bit sequence, which allows deriving the bit error rate (BER) and plotting the eye diagram. For some of the experiments we carried out, the multi-pass cell is removed from the optical path. In that case, the total propagation distance is roughly 2 meters and this corresponds to a back-to-back (B2B) configuration.

3. RESULTS

In the following, mid-infrared transmission results will be shown for two different detection configurations: one with a QWIP, which has a very large bandwidth ($\geq$ 25 GHz[16]) but requires liquid nitrogen and a DC bias, and another one with a QCD, which is a passive room-temperature detector but with a reduced bandwidth (4.5

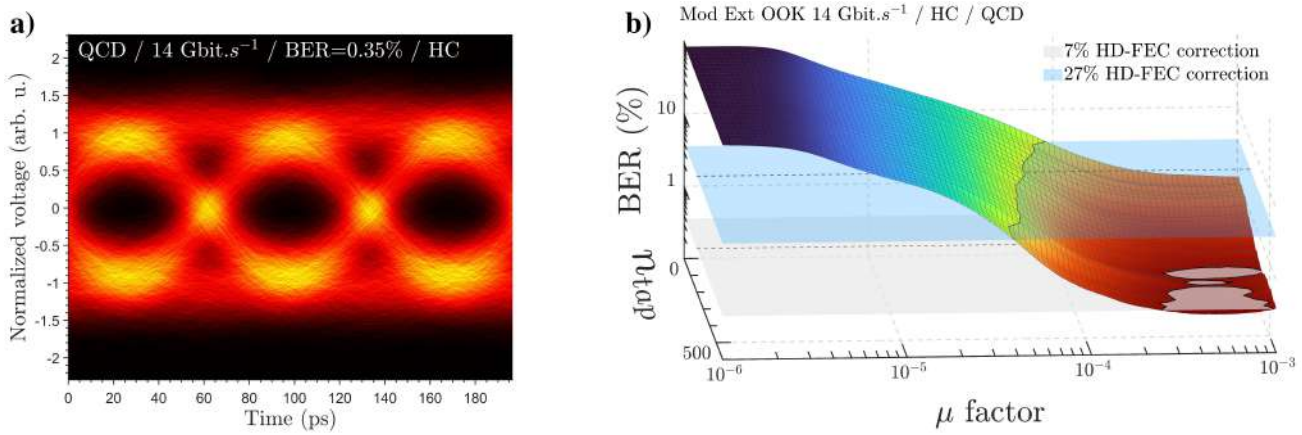

Figure 4. a) Eye diagram of the QCD-scheme transmission after a free-space propagation of approximately 31 meters for an OOK format at 14 Gbit/s, exhibiting an error rate of 0.35 %. b) Optimization of the FFE equalization parameters in order to achieve a BER compatible with either the 27% HD-FEC case or with the 7% HD-FEC case.

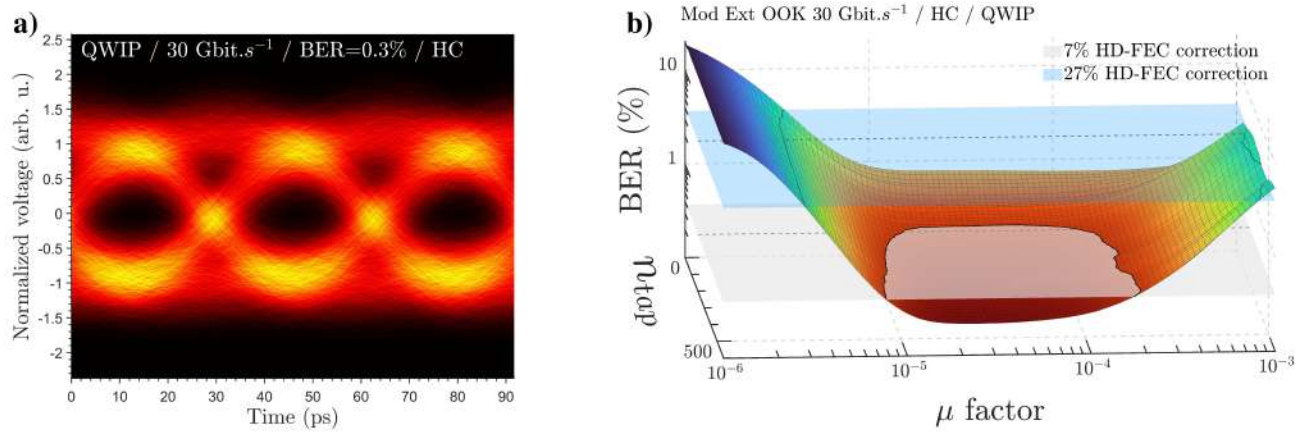

Figure 5. a) Eye diagram of the QWIP-scheme transmission after a free-space propagation of approximately 31 meters for an OOK format at 30 Gbit/s, exhibiting an error rate of 0.3 %. b) Optimization of the FFE equalization parameters in order to achieve a BER compatible with either the 27% HD-FEC case or with the 7% HD-FEC case.

GHz[17]) that limits the maximum speed of the transmission. In addition, experiments were carried out with and without a multi-pass cell to evaluate the degradation of the transmission when increasing the propagation distance (from 2 meters to 31 meters) and when decreasing the amount of optical power reaching the detector. Indeed, mirrors in the multi-pass cell have a high reflectivity of $\simeq$ 98% but the beam is reflected 80 times by these mirrors and consequently, the beam escaping the multi-pass cell is five-time less powerful than the input beam. The pseudorandom binary sequence (PRBS) used for testing the capacity of the transmission channel is a 2-level format (OOK, on-off keying). For each case, we implement a Root-Raised-Cosine (RRC) pulse-shaping filter[18] in order to reduce the spectral occupation of the transmitted signal, and we test the conditions for various roll-off factors to keep the one leading to the minimum BER. At the receiver side, we apply a matched filter, which is an RRC filter with the same roll-off factor. Then, the signal is equalized by using a fractionally-spaced Feed-Forward-Equalization (FFE)[19] at a rate of 4 samples per symbol. The first step of the algorithm learns the coefficients of the channel equalizer by using a least-mean-square gradient descent algorithm with a convergence parameter μ which controls the speed and the accuracy of the learning step. The number of filter coefficients is called n_{tap} and should be large enough to cover all the channel memory. Once the algorithm has converged to achieve an error below a given threshold, the estimated equalizer is applied over the received signal to remove inter-symbol-interference (ISI).

Figure 2 summarizes the results in the case of B2B transmission at 14 Gbit/s with the room-temperature QCD. The left panel shows the eye diagram, which is a convenient tool to quickly assess the quality of the transmission.

To draw this diagram, one has to fold each bit of the received signal into a single pattern. If the eye is wide open (as it is the case in Fig. 2 a)), one can easily discriminate between '0' bits and '1' bits in the received signal. For this first case, a more detailed analysis gives a BER of 0.035%. This value is of interest as it determines if an error-correction code can be used to correct the errors within the received signal and thus achieve an error-free communication. This correction is achieved by adding redundancy bits to the signal that one wants to transmit. In the case of a 7% overhead, the pre-corrected BER can be as high as 0.38% while in the case of a 27% overhead, the pre-corrected BER can be as high as 4% for hard-decision forward error correction (HD-FEC).[20] Figure 2 b) shows the evolution of the BER when tuning the aforementioned parameters n_{tap} and μ. The objective is to find a combination of parameters that complies with one of the two HD-FEC conditions (ideally, the 7% HD-FEC case as the data rate penalty will only be 7%). If several options are available for n_{tap} and μ, choosing the one with the largest μ will ease the implementation as large values lead to faster estimations. For this first B2B configuration at 14 Gbit/s, the target BER $\leq$ 0.38% is achievable for various values of n_{tap} and μ and as aforementioned, the minimum BER one can achieve is actually 0.035%. When one replaces the room-temperature QCD by a cryogenic QWIP in the B2B configuration, it is possible to increase the data rate to 30 Gbit/s while keeping an open eye pattern, as illustrated in Fig. 3 a). This is due to the higher sensitivity and larger bandwidth of the QWIP when compared with the QCD. For this configuration, a limited range of parameters (especially μ) are compatible with an error rate below 0.38%, as shown in Fig. 3 b). The best BER value we were able to achieve for the B2B experiment at 30 Gbit/s is 0.23%.

In order to assess the relevance of our experiment for longer-range free-space transmission, we inserted a multi-pass cell into the optical path and derived the same diagrams at 14 Gbit/s and 30 Gbit/s, for the QCD scheme and the QWIP scheme, respectively. Figure 4 a) shows an open eye pattern, but this eye is not as wide open as the one in the B2B case. Consequently, the BER is much higher and this is attributed to the beam attenuation along the optical path. Yet, the minimum BER in this configuration is 0.35% and this is still compatible with a 7% HD-FEC. Figure 4 b) gives the details of the parameters allowing this low-error rate. Only for particular well-chosen parameters the equalization process leads to a great improvement in terms of transmission quality. Eventually, we also display the best transmission result when both the multi-pass cell and the QWIP are used in Fig. 5. The difference between the B2B and the multi-pass cell is not as important as in the QCD case and this is probably due to the higher sensitivity of QWIP. This higher sensitivity means that this detection system is less affected by the attenuation of the mid-infrared wave along the optical path. Optimization of the signal processing parameters allows reaching a BER as low as 0.3% (Fig. 5 a)), which is consistent with the 7% HD-FEC, and the details for this optimization are found in Fig. 5 b).

4. CONCLUSIONS

This paper highlights the potential of unipolar quantum devices for free space transmissions. It emphasizes the importance of developing equalization processes to significantly increase achievable data rates. Further advancements will focus on implementing unipolar quantum systems in real-world scenarios in multi-km outdoor channels, along with the incorporation of adaptive optics. Additionally, there is room for improvement in the design of unipolar devices to enhance bandwidth and sensitivity. This is especially true for the external modulator and for the detector, as a size reduction of these devices will lead to larger bandwidths.[21] Yet, size reduction also makes the alignment process more complex and one has to find the best compromise in order to combine a high-speed system with sufficient modulated power to achieve long-haul transmission. Last but not least, these findings also pave the way for private free-space communication relying on chaos synchronization[22] that would benefit from external modulators for chaos-masking schemes[23] instead of the current chaos-modulation schemes for QCLs.

Acknowledgments

The authors acknowledge the financial support of the Direction Générale de l'Armement (DGA) and the ENS-Thales Chair. Authors also would like to thank Adel Bousseksou (C2N) for providing the liquid nitrogen.

REFERENCES

[1] R. Martini, R. Paiella, C. Gmachl, F. Capasso, E. Whittaker, H. Liu, H. Hwang, D. Sivco, J. Baillargeon, and A. Cho, "High-speed digital data transmission using mid-infrared quantum cascade lasers," *Electronics Letters* **37**(21), p. 1, 2001.

[2] S. Blaser, D. Hofstetter, M. Beck, and J. Faist, "Free-space optical data link using peltier-cooled quantum cascade laser," *Electronics Letters* **37**(12), pp. 778–780, 2001.

[3] C. Wang, F. Grillot, V. Kovanis, and J. Even, "Rate equation analysis of injection-locked quantum cascade lasers," *Journal of Applied Physics* **113**(6), p. 063104, 2013.

[4] A. Calvar, M. I. Amanti, M. Renaudat St-Jean, S. Barbieri, A. Bismuto, E. Gini, M. Beck, J. Faist, and C. Sirtori, "High frequency modulation of mid-infrared quantum cascade lasers embedded into microstrip line," *Applied Physics Letters* **102**(18), p. 181114, 2013.

[5] X. Pang, O. Ozolins, R. Schatz, J. Storck, A. Udalcovs, J. R. Navarro, A. Kakkar, G. Maisons, M. Carras, G. Jacobsen, *et al.*, "Gigabit free-space multi-level signal transmission with a mid-infrared quantum cascade laser operating at room temperature," *Optics letters* **42**(18), pp. 3646–3649, 2017.

[6] O. Spitz, P. Didier, L. Durupt, D. A. Díaz-Thomas, A. N. Baranov, L. Cerutti, and F. Grillot, "Free-space communication with directly modulated mid-infrared quantum cascade devices," *IEEE Journal of Selected Topics in Quantum Electronics* **28**(1: Semiconductor Lasers), pp. 1–9, 2021.

[7] M. Han, M. Joharifar, M. Wang, Y. Fan, G. Maisons, J. Abautret, Y.-T. Sun, R. Teissier, L. Zhang, V. Bobrovs, *et al.*, "Long-wave infrared discrete multitone free-space transmission using a 9.15-μm quantum cascade laser," *IEEE Photonics Technology Letters* **35**(9), pp. 489–492, 2023.

[8] Y. Su, J. Meng, T. Wei, Z. Xie, S. Jia, W. Tian, J. Zhu, and W. Wang, "150 gbps multi-wavelength fso transmission with 25-ghz itu-t grid in the mid-infrared region," *Optics Express* **31**(9), pp. 15156–15169, 2023.

[9] A. E. Willner, K. Zou, K. Pang, H. Song, H. Zhou, A. Minoofar, and X. Su, "Free-space mid-ir communications using wavelength and mode division multiplexing," *Optics Communications* , p. 129518, 2023.

[10] Q. Lu, S. Slivken, D. Wu, and M. Razeghi, "High power continuous wave operation of single mode quantum cascade lasers up to 5 w spanning λ 3.8-8.3 μm," *Optics Express* **28**(10), pp. 15181–15188, 2020.

[11] L. Durupt, G. Maisons, J. Abautret, M. Guais, R. Teissier, D. Gacemi, A. Vasanelli, and C. Sirtori, "Semiconductor optical amplifier integrated on a single mode quantum cascade laser in the mid-infrared region," in *Novel In-Plane Semiconductor Lasers XXII*, p. PC124400N, SPIE, 2023.

[12] H. Dely, T. Bonazzi, O. Spitz, E. Rodriguez, D. Gacemi, Y. Todorov, K. Pantzas, G. Beaudoin, I. Sagnes, L. Li, *et al.*, "10 gbit s- 1 free space data transmission at 9 μm wavelength with unipolar quantum optoelectronics," *Laser & Photonics Reviews* **16**(2), p. 2100414, 2022.

[13] P. Holmstrom, "High-speed mid-ir modulator using stark shift in step quantum wells," *IEEE journal of quantum electronics* **37**(10), pp. 1273–1282, 2001.

[14] M. Joharifar, H. Dely, X. Pang, R. Schatz, D. Gacemi, T. Salgals, A. Udalcovs, Y.-T. Sun, Y. Fan, L. Zhang, *et al.*, "High-speed 9.6-μm long-wave infrared free-space transmission with a directly-modulated qcl and a fully-passive qcd," *Journal of Lightwave Technology* , 2022.

[15] P. Didier, H. Knötig, O. Spitz, L. Cerutti, A. Lardschneider, E. Awwad, D. Diaz-Thomas, A. Baranov, R. Weih, J. Koeth, *et al.*, "Interband cascade technology for energy-efficient mid-infrared free-space communication," *Photonics Research* **11**(4), pp. 582–590, 2023.

[16] A. Mottaghizadeh, Z. Asghari, M. Amanti, D. Gacemi, A. Vasanelli, and C. Sirtori, "Ultra-fast modulation of mid infrared buried heterostructure quantum cascade lasers," in *2017 42nd International Conference on Infrared, Millimeter, and Terahertz Waves (IRMMW-THz)*, pp. 1–2, IEEE, 2017.

[17] P. Didier, H. Dely, T. Bonazzi, O. Spitz, E. Awwad, E. Rodriguez, A. Vasanelli, C. Sirtori, and F. Grillot, "High-capacity free-space optical link in the midinfrared thermal atmospheric windows using unipolar quantum devices," *Advanced Photonics* **4**(5), p. 056004, 2022.

[18] J. G. Proakis and M. Salehi, *Digital communications*, ch. 3. McGraw-Hill, 2008.

[19] S. Haykin, *Digital communications*, ch. 9. Wiley New York, 1988.

[20] F. Chang, K. Onohara, and T. Mizuochi, "Forward error correction for 100 G transport networks," *IEEE Communications Magazine* **48**(3), pp. S48–S55, 2010.

[21] J. Hillbrand, L. M. Krüger, S. Dal Cin, H. Knötig, J. Heidrich, A. M. Andrews, G. Strasser, U. Keller, and B. Schwarz, "High-speed quantum cascade detector characterized with a mid-infrared femtosecond oscillator," *Optics Express* **29**(4), pp. 5774–5781, 2021.

[22] O. Spitz, A. Herdt, J. Wu, G. Maisons, M. Carras, C.-W. Wong, W. Elsäßer, and F. Grillot, "Private communication with quantum cascade laser photonic chaos," *Nature communications* **12**(1), p. 3327, 2021.

[23] A. Uchida, Y. Liu, and P. Davis, "Characteristics of chaotic masking in synchronized semiconductor lasers," *IEEE journal of quantum electronics* **39**(8), pp. 963–970, 2003.